Molecular Recognition

International Edition: DOI: 10.1002/anie.201503948
German Edition: DOI: 10.1002/ange.201503948

Force Spectroscopy of Metal–Crown Ether Multivalency: Effect of Local Environments on Energy Landscape and Sensing Kinetics**

*Ting-Yang Kuo, Wei-Hsiang Tseng, and Chun-hsien Chen**

Abstract: *Sandwich complexation involving alkali or alkaline-earth metals, multivalency, and effects associated with local environments is widely encountered in biological and synthetic systems yet the mechanic properties remain unexplored. Herein, AFM (atomic force microscopy)-based single-molecule force spectroscopy is employed to investigate a classical model of $M^{n+}[15C5]_2$, a metal cation hosted jointly by two 15-crown-5 moieties immobilized on both the substrate and the AFM tip. Factors reportedly promoting the recognition performance are examined. The rupture force required to break apart $M^{n+}[15C5]_2$ is found to be in the order of tens of pico-Newton, e.g., $f_\beta = 31$ pN for $K^+[15C5]_2$. The presence of a second functional group, carboxylate, confers $K^+[15C5]_2$ with a longer lifetime (from 13 to 16 ms), faster association (from 0.4 to 1.3×10^6 $M^{-1} s^{-1}$), and slower dissociation (from 77 to 62 s^{-1}). The effect of local environments is significant on association yet less critical on dissociation pathways.*

Molecular recognition through reversible noncovalent and multivalent interactions operating collectively with neighboring functionalities is one of the most significant features of chemical and biological systems. Among the sensing elements and synergistically acting components, moieties of crown ethers[1–3] have long been acknowledged and are still actively involved in contemporary challenges; to name a few: ion-channel transport,[4–6] modulating protein surface properties,[7] monitoring the motion of a guest molecule on a multitopic host,[8,9] template-assisted synthesis,[2,10–13] switchable performance in catalysis[14,15] and in molecular machines,[12,13,16,17] and energy storage.[18] To achieve these tasks effectively and repeatedly, reversible dissociation that restores the host configuration is as important as the step of associative recognition. However, the mechanical nature to evaluate the reversibility for metal–crown ether complexes has yet been reported. Further surprisingly, literature work on thermodynamic and kinetic parameters in the solution phase[19] is scarce for the famous sandwich complexes, $M^{n+}[crown]_2$, that have been utilized in many phenomenal sensing applications.[20] Taking advantage of AFM-based (atomic force microscopy) single-molecule force spectroscopy,[21–23] we will quantitatively show here the mechanic strengths, free-energy landscapes, and the kinetic parameters of the dissociation of metal–crown ether complexes.

The model system is $M^{n+}[15C5]_2$ and the experimental concept is illustrated in Figure 1 A with moieties of 15-crown-5 ether immobilized on Au substrate by sulfur–gold (RS-Au)

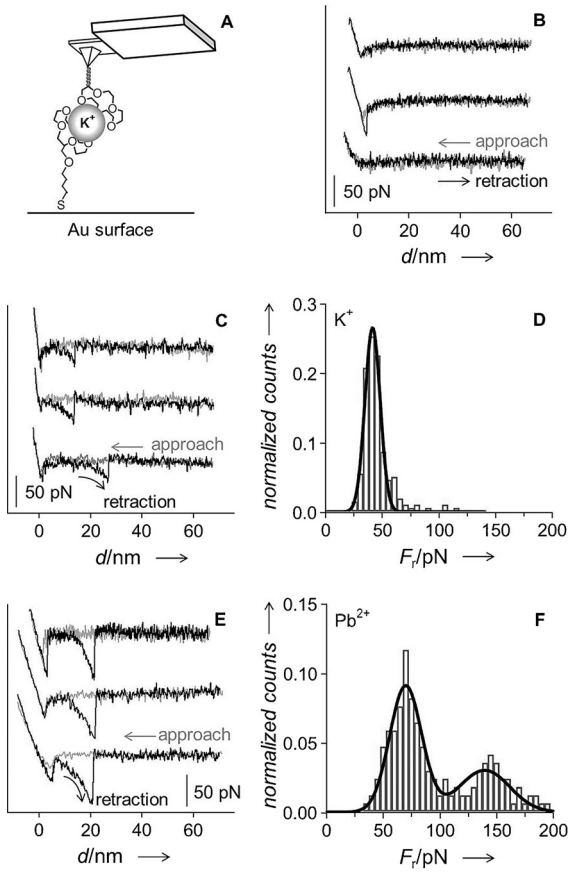

Figure 1. Single-molecule force spectroscopy for crown–metal–crown complexations. A) Presentation of AFM-based measurements. The illustration is not drawn to scale. Typical force traces and corresponding histograms of unbinding forces obtained in aqueous solutions of B) blank, C,D) 0.5 mM K^+, and E,F) 0.5 mM Pb^{2+}. The grey and black traces indicate the directions of tip approaching toward and retracting from the substrate, respectively. To prepare panels D and F, acquired for each case are 1000 force–distance traces in which 226 traces exhibit rupture forces for the former and 203 traces for the latter. The solid curves are Gaussian fitting from which the peak positions were determined. The bin width of unbinding forces in the histograms is 5 pN. Force measurements were performed with a loading rate of 10.5 nN s^{-1} (with an apparent spring constant of 0.035 nN nm^{-1} and a retraction velocity of 300 nm s^{-1}).

[*] Dr. T.-Y. Kuo, Dr. W.-H. Tseng, Prof. Dr. C.-h. Chen
Department of Chemistry and Center for Emerging Material and Advanced Device, National Taiwan University
1, Sec. 4, Roosevelt Road, Taipei, 10617 (Taiwan)
E-mail: chhchen@ntu.edu.tw

[**] This study was financially supported by National Taiwan University, MOE, and MOST. The authors thank Fung-Mei Chen and Yao-Wen Chang for the preparation of the TOC graphic.

Supporting information for this article is available on the WWW under http://dx.doi.org/10.1002/anie.201503948.

adsorption and on the Si_3N_4 AFM tip by the covalent carbon–silicon (RC-OSi) bond through a polyethylene glycol (PEG) chain.[24] The PEG chain is a flexible spacer and is introduced to differentiate specific crown–metal–crown ($M^{n+}[15C5]_2$) interactions from the nonspecific ones arising from substrate–tip physisorption. Examples for the latter are displayed in Figure 1 B, in which the force–distance traces are obtained from a blank solution free of metal cations. Nonspecific physisorption is located around zero extension of the *z*-piezoelectrics and is characterized as an attractive force. The bottom trace in Figure 1 B manifests force curves that bear insignificant nonspecific adhesion. Such features are observed quite often ($\approx$60 %) and are strongly dependent on local environments because, under the conditions of blank tests, the discrepancy among different sampling locations appears drastic.

With the presence of metal cations, the approaching of the tip toward the substrate may lead to complexation of one metal cation sandwiched by two 15C5 moieties (Figure 1 A). The subsequent tip retraction would result in observable rupture forces. For example, panels C and E are obtained in solutions containing K^+ and Pb^{2+}, respectively. In addition to the physisorption signature, the retraction traces exhibit rupture events corresponding to the breaking of the sandwich complexes. The rupture force takes place at a larger piezo extension due to the incorporation of the stretchy PEG chain. Panels D and F summarize the force distributions with the most probable peaks at 41($\pm$7) pN and 70($\pm$14) pN, respectively. The values are two orders of magnitude weaker than those required to disrupt the linkers of crown moieties from the tip or substrate. Specifically, it takes about 3.0 nN to break a Si–O bond,[25] and ca. 0.5–1.5 nN to remove thiols from a gold surface.[26–28] Therefore, the rupture forces in Figure 1 D and F are attributed to those of the multivalent crown–metal–crown interactions.

The same procedures are carried out for alkali and alkaline earth metals (Figure S2). For the cases of Na^+ and Mg^{2+}, no apparent rupture force can be determined. It is known that crown–cation complexation is sensitive to d_{metal}/d_{crown}, the ratio of cation diameters[29] to the size of 15-crown-5 cavity ($\approx$0.202 nm).[30] Indeed, the rupture force correlates strongly with the size ratio (Figure 2). Only with d_{metal} larger than d_{crown} can the rupture force be found, consistent with the criteria for the formation of sandwich complexes.[31,32] The ratio of ca. 1.2 confers the largest rupture force. A bigger cation deviates the crown moiety from the optimal chelating conformation and reduces the required rupture force. In addition, divalent cations, e.g., Pb^{2+} and Ba^{2+}, exhibit stronger rupture forces than the monovalent ones.

It is well known that the formation constants of crown–metal complexes in organic solvents are orders of magnitude higher than those in aqueous solutions because of the uncomplimentary conformation developed for the latter. Accordingly, this study examines the dependence of rupture forces on solvent polarity for sandwich complexes of K^+ and Pb^{2+} (Figure S3). The obtained values for K^+ are 41($\pm$7), 45($\pm$8), and 46($\pm$10) pN in water, methanol, and acetonitrile, respectively, whereas the values for Pb^{2+} are 70($\pm$14), 72($\pm$15), 70($\pm$21) pN, respectively. The rupture force and thus the strength of metal–crown ether coordination are essentially independent on solvent polarity.

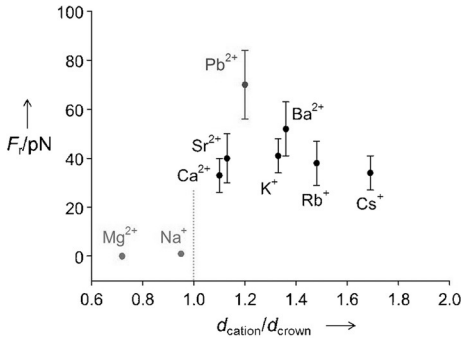

Figure 2. Rupture force plotted against the size ratio of the metal cation and the crown cavity. The rupture forces for Na^+ and Mg^{2+} are unobservable. All experiments were conducted in aqueous solutions containing chloride salt of the corresponding analyte cation (0.5 mM). The values of rupture force for K^+, Rb^+, Cs^+, Ca^{2+}, Sr^{2+}, Ba^{2+}, and Pb^{2+} are 41($\pm$7), 38($\pm$9), 34($\pm$7), 33($\pm$7), 40($\pm$10), 52($\pm$11), and 70($\pm$14) pN, respectively. Other conditions are the same as those of Figure 1.

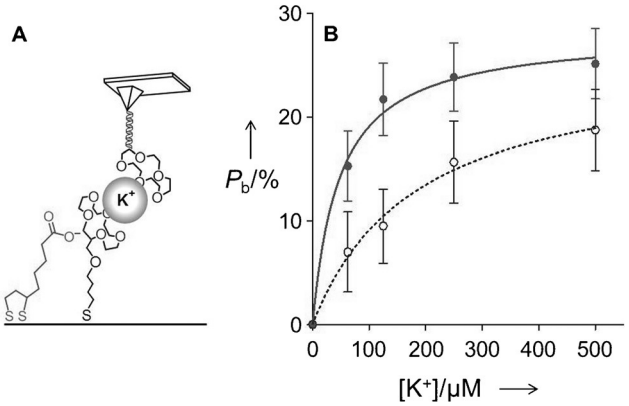

Figure 3. A) Illustration for the crown moiety preorganized due to the repulsion from neighboring carboxylate groups. B) Isotherms of binding probability (P_b) for $K^+[15C5]_2$ sandwich interactions on substrate modified by 15C5-C_4-SH only (dot curve, open circles) and co-assembled with thioctic acid (solid curve and circles). The curves show data fitting to the model of Langmuir isotherm. Other conditions are the same as those of Figure 1.

To further explore the effect of local environments, 15C5-C_4-SH and thioctic acid (TA) are co-assembled on gold substrate (Figure 3 A). The experiments are designed according to our previous studies[33–37] of nanoparticle-based colorimetric sensing in which aggregation of 15C5-modified nanoparticles is triggered by sandwiched $K^+[15C5]_2$.[38] The sensing performance is significantly improved by the presence of TA, ascribed to 1) an increased local concentration of K^+ attracted electrostatically by the carboxylates and 2) preorganized crown moieties due to the electrostatic repulsion between the oxygen atoms and the neighboring carboxylates.[34] In the present study, Figure 3 B shows that the introduction of TA (solid circles) raises the binding probability of rupture events. The probability appears unaffected by ionic strength. Specifically, for cases with a fixed concentration of K^+ at 62.5 μM, P_b

remains nominally at 15% when the solution contains additional NaCl ranging from 0 to 0.43 mM (Figure S4).

Both cases, with and without the co-assembled TA, show the behavior of binding saturation. Hence, Figure 3 presents isotherms of binding probability (P_b) fitted to the Langmuir-type model for specific binding.[39,40]

$$\frac{P_b}{P_{b,max}} = \frac{K_A[K^+]}{1+K_A[K^+]} = \frac{[K^+]}{(1/K_A)+[K^+]} = \frac{[K^+]}{K_D+[K^+]} \quad (1)$$

in which $P_{b,max}$ is the maximum (i.e., saturated) binding probability and K_A (K_D) is the apparent association (dissociation) constant. The values of K_A (Table 1) are thus deduced from the fitting. For substrates with co-presence of 15C5 and TA, K_A is $20.9(\pm 4.3)\times 10^3\,M^{-1}$, about four times that with 15C5 alone. The superior affinity for the former is consistent with the aforementioned models proposing that carboxylates of TA attract K^+ electrostatically or facilitate the formation of preorganized crown moieties.

Gibbs free energy for the dissociation of the $K^+[15C5]_2$ sandwich complex is estimated by $\Delta G = -RTlnK_D$. The results show that ΔG for $K^+[15C5]_2$ being dissociated from the co-assembled environment takes 24.7 kJ mol^{-1} and 21.3 kJ mol^{-1} from substrate modified by crown only (Figure 5), demonstrating that the co-presence of carboxylates stabilizes the sandwich complexes. Also displayed for comparison is an unstressed ΔG of 32.2 kJ mol^{-1}, deduced from an ab initio computational study.[41]

Note that the rupture force (F_r), instead of being a constant value, is logarithmically dependent on the velocity of tip retraction (v_{tip}) and thus the loading rate (r_{appl}, pN/s; r_{appl} = (apparent spring constant) × v_{tip}). r_{appl} corresponds to the force applied within a certain timespan.[42] A larger r_{appl} skews the Gibbs free-energy landscape more significantly, leading to a shorter lifetime and a larger rupture force.[43–45] To learn the dissociation pathway for $K^+[15C5]_2$ without being subject to the external mechanical stress (hereafter referred to as "at zero force"), dynamic force spectroscopy was carried out (Figure 4). Based on the Bell–Evans approach,[21,46,47] the F_r–r_{appl} correlation can be formulated by Equation (2).

$$F_r(r_{appl}) = f_\beta ln(r_{appl}/r^0{}_{appl}) = f_\beta ln(r_{appl}) - f_\beta ln(r^0{}_{appl}) \quad (2)$$

The semi-logarithmic plot gives the slope (f_β) and the intercept ($r^0{}_{appl}$). Both f_β and $r^0{}_{appl}$ are associated with the properties at zero force. Explicitly, f_β is termed thermal fluctuation force to describe what is required to dissociate $K^+[15C5]_2$ at zero force. Derived from $E_{thermal} = k_BT = f_\beta x_\beta$, the width of the energy barrier (x_β, see Figure 5) further elaborates the free-energy landscape for the complex going from the equilibrium position of the complex to the transition state. Similarly, at zero force, $r^0{}_{appl}$ is equivalent to the loading rate driven by the environmental thermal energy. By taking advantage of the correlation of the loading rate with lifetime (τ^0, $r^0{}_{appl} = k_BT/\tau^0$) and dissociation rate (k_{off}, $k_{off} = 1/\tau^0$), the values of τ^0 and k_{off} for $K^+[15C5]_2$ at zero force can be found (Table 1).

Figure 4 shows the F_r–$ln(r_{appl})$ plot across three orders of magnitude. The extracted parameters are summarized in

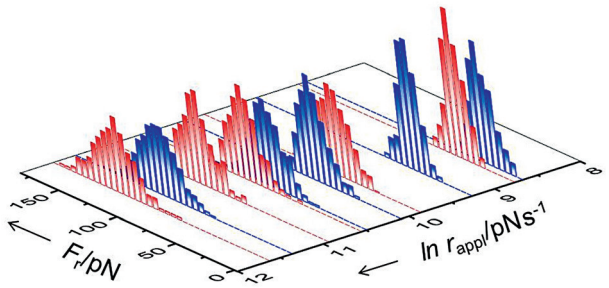

Figure 4. Dynamic force spectroscopy on substrates modified by 15C5-C_4-SH alone (blue) and co-assembled with TA (red). The histograms of rupture forces are plotted against the loading rates and yield slopes (f_β) with essentially the same values (31 pN). The loading rates range from 5.8 to 125 nN s^{-1}. To plot the histograms, utilized traces are limited to those with single polymeric molecule force traces screened by the worm-like chain model[22,48] (see the Supporting Information for details).

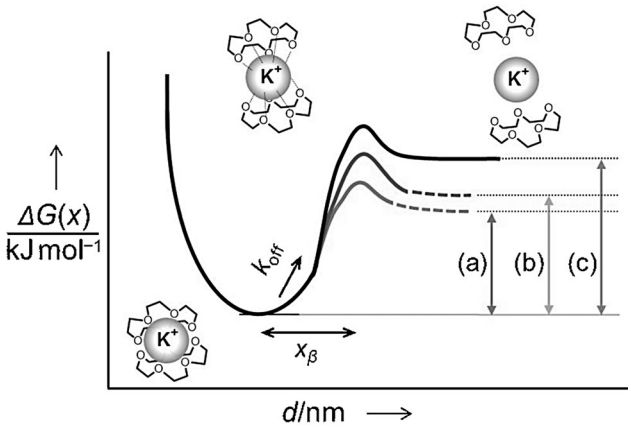

Figure 5. Illustration of the energy landscapes for $K^+[15C5]_2$. x_β is found 0.13 nm for cases with and without co-assembly of TA. ΔG for the dissociation of $K^+[15C5]_2$ a) from substrate modified by crown only is 21.3 kJ mol^{-1}, b) from substrate co-assembled with TA is 24.7 kJ mol^{-1}, and c) from simulated result[41] is 32.2 kJ mol^{-1}. The values of k_{off} are summarized in Table 1. For better comparison of the free energies, the minima of the potential wells are aligned for clarity.

Table 1: Effect of local environments on equilibrium and kinetic parameters for $K^+[15C5]_2$ sandwich interactions.

Local environment	K_D [μM][a]	K_A [$\times 10^3$ M^{-1}][a]	f_β [pN][b]	x_β [Å][b]	$r^0{}_{appl}$ [pN s^{-1}][b]	τ^0 [ms][c]	k_{off} [s^{-1}][c]	k_{on} [$\times 10^6$ M^{-1} s^{-1}][c]
crown alone	186(±45)	5.4(±1.3)	31.2(±1.1)	1.32(±0.04)	2397	13.0(±0.5)	77.0(±2.7)	0.41(±0.10)
crown + TA	47.8(±9.8)	20.9(±4.3)	30.5(±1.6)	1.35(±0.07)	1897	16.1(±0.8)	62.2(±3.3)	1.30(±0.27)

[a] K_D and K_A are derived from isotherms of binding probability (Figure 3) and are multiplicative inverses of each other. [b] f_β and $r^0{}_{appl}$ are calculated from the plots of loading rate against rupture force (Figure 4). x_β is obtained by $E_{thermal} = k_BT = f_\beta x_\beta$. [c] Lifetime ($\tau^0$) and dissociate rate ($k_{off}$) are derived from $r^0{}_{appl}$ ($r^0{}_{appl} = f_\beta x_\beta/\tau^0 = (k_BT)k_{off}$) and are reciprocals. k_{on} is obtained by $K_A = k_{on}/k_{off}$.

Table 1 and Figure 5. For both conditions, without or with the co-assembly of TA, the properties associated with mechanical rupturing are essentially the same, such as thermally induced f_β and x_β. The derived barrier width, x_β ($\approx$0.13 nm), is on the same order of magnitude as the simulated K^+–O distance (0.183 nm) for $K^+[15C5]_2$ reported in a DFT study.[49]

The presence of TA enables $K^+[15C5]_2$ one-quarter extension in lifetime (τ^0), three-fold acceleration in the formation rate (k_{on}), and a decrease in the dissociation rate (k_{off}). The seemingly rapid k_{off} of 62.2 and 77.0 s^{-1} is in fact comparable to that of supramolecular complexes (e.g., 7.6–50 s^{-1} for the urea–aminotriazine pair[50,51]) and that of cell adhesion proteins (7–200 s^{-1}).[52–54] The values of k_{off} for $K^+[15C5]_2$ are actually orders of magnitude lower than those of 1-to-1 M^{n+}[crown] complexation (10^2–10^7 s^{-1}).[20,55,56] The slow k_{off} of $K^+[15C5]_2$ is attributed to the sandwich configuration in which two halves of concaved 15C5 moieties enclose K^+ through multivalent binding. For the dissociation of $K^+[15C5]_2$, such conformation impedes the access of solvent molecules to interact with the crown-coordinated metal center and diminishes the influence from proximal environments. Therefore, under external mechanical stress, the rupture force is independent of solvent polarity (Figure S3) and f_β is essentially the same for 15C5-modified substrate with and without TA (i.e., the slope of dynamic force spectroscopy, Figure 4). The results show quantitatively that the effect of local environments is significant on association kinetics yet less critical on dissociation reactions.

In conclusion, the mechanical strength of multivalent crown–metal interactions is determined quantitatively by single-molecule force spectroscopy. Regarding the dissociation reaction, the external force required to break apart the sandwich complexes has the following features. The magnitude is 1) on the order of tens of pN, comparable to that of carbohydrate–receptor pairs (e.g., lactose–IgG[57] or ganglioside G_{M1}–cholera toxin B[58]), 2) dependent on the oxidation number and the size ratio of the metal diameter to the crown cavity, and 3) independent of solvent polarity. Through isotherms of binding probability and dynamic force spectroscopy, the free-energy landscapes and kinetic parameters for the dissociation of $K^+[15C5]_2$ are derived based on the Bell–Evans model. For 15C5-modified substrate with and without co-assembled carboxylate groups, the values of rupturing force (f_β) are similar under external mechanical stress. The one-quarter difference in loading rate (r^0_{appl}) and lifetime (τ^0) can only be apparent at zero force. Regarding the association reaction, the presence of carboxylates accelerates the complexation, attributed to the development of electrostatic attractions toward K^+ and/or conformational pre-organization of neighboring crown moieties. The rates of association and dissociation are, respectively, 3-fold faster and one-quarter-slower than those with 15C5 alone. These findings provide mechanical and kinetic information on the mechanism of sandwich complexations. The quantitative results elucidate the importance of local environments on recognition and sensing performance for the design of reaction schemes.

Keywords: crown compounds · ion-molecule reactions · kinetics · molecular recognition · sandwich complexes

How to cite: *Angew. Chem. Int. Ed.* **2015**, *54*, 9213–9217
Angew. Chem. **2015**, *127*, 9345–9349

[1] H.-J. Schneider, A. K. Yatsimirsky, *Chem. Soc. Rev.* **2008**, *37*, 263–277.
[2] T. Terashima, M. Kawabe, Y. Miyabara, H. Yoda, M. Sawamoto, *Nat. Commun.* **2013**, *4*, 2321.
[3] J. Guo, J. Lee, C. I. Contescu, N. C. Gallego, S. T. Pantelides, S. J. Pennycook, B. A. Moyer, M. F. Chisholm, *Nat. Commun.* **2014**, *5*, 5389.
[4] C. D. Assouma, A. Crochet, Y. Chérémond, B. Giese, K. M. Fromm, *Angew. Chem. Int. Ed.* **2013**, *52*, 4682–4685; *Angew. Chem.* **2013**, *125*, 4780–4783.
[5] T. Saha, S. Dasari, D. Tewari, A. Prathap, K. M. Sureshan, A. K. Bera, A. Mukherjee, P. Talukdar, *J. Am. Chem. Soc.* **2014**, *136*, 14128–14135.
[6] F. Otis, M. Auger, N. Voyer, *Acc. Chem. Res.* **2013**, *46*, 2934–2943.
[7] C.-C. Lee, M. Maestre-Reyna, K.-C. Hsu, H.-C. Wang, C.-I. Liu, W.-Y. Jeng, L.-L. Lin, R. Wood, C.-C. Chou, J.-M. Yang, A. H.-J. Wang, *Angew. Chem. Int. Ed.* **2014**, *53*, 13054–13058; *Angew. Chem.* **2014**, *126*, 13270–13274.
[8] D. P. Weimann, H. D. Winkler, J. A. Falenski, B. Koksch, C. A. Schalley, *Nat. Chem.* **2009**, *1*, 573–577.
[9] H. D. Winkler, D. P. Weimann, A. Springer, C. A. Schalley, *Angew. Chem. Int. Ed.* **2009**, *48*, 7246–7250; *Angew. Chem.* **2009**, *121*, 7382–7386.
[10] Y.-H. Lin, C.-C. Lai, Y.-H. Liu, S.-M. Peng, S.-H. Chiu, *Angew. Chem. Int. Ed.* **2013**, *52*, 10231–10236; *Angew. Chem.* **2013**, *125*, 10421–10426.
[11] R. E. Mulvey, F. Mongin, M. Uchiyama, Y. Kondo, *Angew. Chem. Int. Ed.* **2007**, *46*, 3802–3824; *Angew. Chem.* **2007**, *119*, 3876–3899.
[12] S. F. van Dongen, S. Cantekin, J. A. Elemans, A. E. Rowan, R. J. Nolte, *Chem. Soc. Rev.* **2014**, *43*, 99–122.
[13] C. J. Bruns, J. F. Stoddart, *Acc. Chem. Res.* **2014**, *47*, 2186–2199.
[14] G. H. Ouyang, Y. M. He, Y. Li, J. F. Xiang, Q. H. Fan, *Angew. Chem. Int. Ed.* **2015**, *54*, 4334–4337; *Angew. Chem.* **2015**, *127*, 4408–4411.
[15] M. R. Kita, A. J. Miller, *J. Am. Chem. Soc.* **2014**, *136*, 14519–14529.
[16] V. N. Vukotic, K. J. Harris, K. Zhu, R. W. Schurko, S. J. Loeb, *Nat. Chem.* **2012**, *4*, 456–460.
[17] P. Lussis, T. Svaldo-Lanero, A. Bertocco, C.-A. Fustin, D. A. Leigh, A.-S. Duwez, *Nat. Nanotechnol.* **2011**, *6*, 553–557.
[18] D.-W. Lim, S. A. Chyun, M. P. Suh, *Angew. Chem. Int. Ed.* **2014**, *53*, 7819–7822; *Angew. Chem.* **2014**, *126*, 7953–7956.
[19] To the best of our knowledge, there are only three studies reporting the thermodynamic constants for sandwich complexes of $M^{n+}[crown]_2$. The experiments were carried out for K^+-[crown]$_2$ with the second-step association constant, K_{A2}, of 9.5×10^2[19a], 2.7×10^3 M^{-1}[19b] in water, 5.6×10^2 in acetonitrile,[19c] and 6.9×10^2 M^{-1} in propylene carbonate.[19c] a) Y. Liu, L.-H. Tong, Y. Inoue, T. Hakushi, *J. Chem. Soc. Perkin Trans. 2* **1990**, 1247–1253; b) G. W. Liesegang, M. M. Farrow, N. Purdie, E. M. Eyring, *J. Am. Chem. Soc.* **1976**, *98*, 6905–6908; c) H.-J. Buschmann, *Polyhedron* **1988**, *7*, 721–724.
[20] G. W. Gokel, W. M. Leevy, M. E. Weber, *Chem. Rev.* **2004**, *104*, 2723–2750.
[21] R. Merkel, P. Nassoy, A. Leung, K. Ritchie, E. Evans, *Nature* **1999**, *397*, 50–53.
[22] A. Janshoff, M. Neitzert, Y. Oberdörfer, H. Fuchs, *Angew. Chem. Int. Ed.* **2000**, *39*, 3212–3237; *Angew. Chem.* **2000**, *112*, 3346–3374.

[23] F. A. Carvalho, N. C. Santos, *IUBMB life* **2012**, *64*, 465 – 472.
[24] D. C. Klein, C. M. Stroh, H. Jensenius, M. van Es, A. Kamruzzahan, A. Stamouli, H. J. Gruber, T. H. Oosterkamp, P. Hinterdorfer, *ChemPhysChem* **2003**, *4*, 1367 – 1371.
[25] M. K. Beyer, *J. Chem. Phys.* **2000**, *112*, 7307 – 7312.
[26] B. Xu, X. Xiao, N. J. Tao, *J. Am. Chem. Soc.* **2003**, *125*, 16164 – 16165.
[27] X. Li, J. He, J. Hihath, B. Xu, S. M. Lindsay, N. Tao, *J. Am. Chem. Soc.* **2006**, *128*, 2135 – 2141.
[28] Y. Xue, X. Li, H. Li, W. Zhang, *Nat. Commun.* **2014**, *5*, 4348.
[29] L. H. Ahrens, *Geochim. Cosmochim. Acta* **1952**, *2*, 155 – 169.
[30] M. Ouchi, Y. Inoue, T. Kanzaki, T. Hakushi, *J. Org. Chem.* **1984**, *49*, 1408 – 1412.
[31] I.-H. Chu, H. Zhang, D. V. Dearden, *J. Am. Chem. Soc.* **1993**, *115*, 5736 – 5744.
[32] J. W. Steed, J. L. Atwood, *Supramolecular Chemistry*, Wiley, New York, **2000**.
[33] S.-Y. Lin, S.-H. Wu, C.-h. Chen, *Angew. Chem. Int. Ed.* **2006**, *45*, 4948 – 4951; *Angew. Chem.* **2006**, *118*, 5070 – 5073.
[34] S.-Y. Lin, C.-h. Chen, M.-C. Lin, H.-F. Hsu, *Anal. Chem.* **2005**, *77*, 4821 – 4828.
[35] S.-Y. Lin, S.-W. Liu, C.-M. Lin, C.-h. Chen, *Anal. Chem.* **2002**, *74*, 330 – 335.
[36] S.-H. Wu, Y.-S. Wu, C.-h. Chen, *Anal. Chem.* **2008**, *80*, 6560 – 6566.
[37] S.-Y. Lin, Y.-T. Tsai, C.-C. Chen, C.-M. Lin, C.-h. Chen, *J. Phys. Chem. B* **2004**, *108*, 2134 – 2139.
[38] M.-L. Ho, J.-M. Hsieh, C.-W. Lai, H.-C. Peng, C.-C. Kang, I.-C. Wu, C.-H. Lai, Y.-C. Chen, P.-T. Chou, *J. Phys. Chem. C* **2009**, *113*, 1686 – 1693.
[39] W. Baumgartner, P. Hinterdorfer, W. Ness, A. Raab, D. Vestweber, H. Schindler, D. Drenckhahn, *Proc. Natl. Acad. Sci. USA* **2000**, *97*, 4005 – 4010.
[40] I. H. Kim, M. N. Lee, S. H. Ryu, J. W. Park, *Anal. Chem.* **2011**, *83*, 1500 – 1503.
[41] M. Saiful Islam, R. A. Pethrick, D. Pugh, M. J. Wilson, *J. Chem. Soc. Faraday Trans.* **1998**, *94*, 39 – 46.
[42] W. Zhang, X. Lü, W. Zhang, J. Shen, *Langmuir* **2011**, *27*, 15008 – 15015.
[43] O. K. Dudko, *Proc. Natl. Acad. Sci. USA* **2009**, *106*, 8795 – 8796.
[44] E. A. Evans, D. A. Calderwood, *Science* **2007**, *316*, 1148 – 1153.
[45] P. Samorì, *Scanning Probe Microscopies beyond Imaging: Manipulation of Molecules and Nanostructures*, Wiley, Hoboken, **2006**.
[46] E. Evans, K. Ritchie, *Biophys. J.* **1997**, *72*, 1541 – 1555.
[47] J. T. Bullerjahn, S. Sturm, K. Kroy, *Nat. Commun.* **2014**, *5*, 4463.
[48] M. I. Giannotti, G. J. Vancso, *ChemPhysChem* **2007**, *8*, 2290 – 2307.
[49] B. Martínez-Haya, P. Hurtado, A. R. Hortal, J. D. Steill, J. Oomens, P. J. Merkling, *J. Phys. Chem. A* **2009**, *113*, 7748 – 7752.
[50] A. Embrechts, H. Schönherr, G. J. Vancso, *J. Phys. Chem. B* **2012**, *116*, 565 – 570.
[51] A. Embrechts, A. H. Velders, H. Schönherr, G. J. Vancso, *Langmuir* **2011**, *27*, 14272 – 14278.
[52] X. Zhang, E. Wojcikiewicz, V. T. Moy, *Biophys. J.* **2002**, *83*, 2270 – 2279.
[53] K. K. Sarangapani, T. Yago, A. G. Klopocki, M. B. Lawrence, C. B. Fieger, S. D. Rosen, R. P. McEver, C. Zhu, *J. Biol. Chem.* **2004**, *279*, 2291 – 2298.
[54] E. Evans, A. Leung, V. Heinrich, C. Zhu, *Proc. Natl. Acad. Sci. USA* **2004**, *101*, 11281 – 11286.
[55] J. K. Rasmussen, S. M. Heilmann, P. E. Toren, A. V. Pocius, T. A. Kotnour, *J. Am. Chem. Soc.* **1983**, *105*, 6845 – 6849.
[56] C. D. Geary, S. G. Weber, *Anal. Chem.* **2003**, *75*, 6560 – 6565.
[57] W. Dettmann, M. Grandbois, S. André, M. Benoit, A. K. Wehle, H. Kaltner, H.-J. Gabius, H. E. Gaub, *Arch. Biochem. Biophys.* **2000**, *383*, 157 – 170.
[58] X.-E. Cai, J. Yang, *Biochemistry* **2003**, *42*, 4028 – 4034.

Received: April 30, 2015
Published online: June 18, 2015

